Analysis and Development of Fixed and Variable Waveband MUX/DEMUX Utilizing AWG Routing Functions

Shoji Kakehashi, Hiroshi Hasegawa, *Member, IEEE*, Ken-ichi Sato, *Fellow, IEEE*, Osamu Moriwaki, *Member, IEEE*, and Shin Kamei

***Abstract*—We develop and analyze a new waveband multi/demultiplexer that exploits the routing functions of arrayed-waveguide gratings (AWG). The device can accommodate multiple input/output fibers simultaneously and be implemented monolithically using silica planar lightwave circuit (PLC) technology. We analyze AWG port usage for variants of the proposed multi/demultiplexers. The important characteristic of the device, its coherent and incoherent crosstalk performance is investigated. A technique to reduce the crosstalk is presented. We extend the capability of the device so that the waveband bandwidth can be changed by adding small switches. Experiments confirm the excellent performance of the proposed waveband multi/demultiplexer.**

***Index Terms*—Arrayed-waveguide gratings (AWG), crosstalk, planar lightwave circuit (PLC), waveband, waveband cross connect, waveband multi/demultiplexer (MUX/DEMUX).**

I. Introduction

INTERNET traffic is continually increasing spurred by the rapid penetration of broadband access such as ADSL and FTTH throughout the world. To cope with this, wavelength routing using the reconfigurable optical add-drop multiplexer (ROADM) is being widely adopted to develop cost-effective metro networks [1]. Generalized multprotocol label switch (GMPLS) controlled optical path cross connects (OXCs) have also been used to create nationwide testbeds [2]. The maximum number of wavelengths (optical paths) per fiber now exceeds 100. Further traffic expansion is expected in the near future with the introduction of new broadband services including IP TV and IP-based high definition TV. This will result in a significant increase in the number of wavelength paths that are to be cross connected at nodes, and, hence, optical node throughput needs to be greatly enhanced at reasonable cost. To resolve this problem, the hierarchical optical path architecture and the hierarchical OXC (HOXC) [3]–[9] are being actively investigated; they can switch hierarchical bandwidth optical paths, wavelength paths and wavebands that consist of multiple wavelength paths. Indeed, several studies have targeted the development of hierarchical optical path network design algorithms [10]–[12], and have demonstrated the advantage of introducing HOXCs; most of the works evaluated the effectiveness in terms of the total number of OXC and HOXC ports compared to those of single-layer OXCs. Another study [13] showed that an HOXC with nonuniform waveband size cannot only improve node throughput but also reduce cross-connect node cost.

Various node and switch architectures for HOXC were studied in [7], which demonstrated that switch size can be greatly reduced by employing wavebands. The HOXC consists of new key components, waveband cross connect (BXC) and waveband multi/demultiplexer (MUX/DEMUX). Some architectures for waveband MUX/DEMUX have been proposed. A dielectric multilayer filter has been reported that offers 8-skip-0 band operation supporting a total of 32 channels at 100-GHz spacing [14]. It requires 409 layers [14] and the manufacturing challenge is significant. Another band filter that consists of two specially designed arrayed-waveguide gratings (AWGs) has been reported [15], [16]. They reported an 8-skip-0 band configuration with a total of 40 channels and 100-GHz spacing [16]. The output/input ports of the two AWGs need to be connected with waveguides of exactly the same length so device size tends to be large. A more recent proposal [17] uses concatenated conventional AWGs to realize a waveband MUX/DEMUX. The key to the waveband MUX/DEMUX is that it retains multi/demultiplexing granularity at the individual wavelength channel level. The AWGs are thus conventional ones whose wavelength channel resolution matches the International Telecommunication Union (ITU-T) grid. The length of each waveguide/fiber connecting the two AWGs is arbitrary and hence the device can be smaller due to the inherent layout flexibility. Indeed, the device so fabricated [18], [19] adopted a folded layout of two AWGs to reduce chip size (and, hence, necessary substrate size). The other salient feature of the waveband MUX/DEMUX is that it can accommodate multiple input fibers simultaneously and demultiplex each band to different output ports, which makes it very effective in reducing BXC cost and size (see Fig. 1). One potential deficiency of the proposed waveband MUX/DEMUX is its susceptibility to the filtering effect since each waveband MUX/DEMUX basically

Manuscript received March 9, 2008; revised July 3, 2008. Current version published February 13, 2009. This work was supported in part by the Japan Science and Technology Agency (JST).

S. Kakehashi, H. Hasegawa, and K. Sato are with Nagoya University, Nagoya 464-8603, Japan (e-mail: s_kakeha@echo.nuee.nagoya-u.ac.jp; hasegawa@nuee.nagoya-u.ac.jp; sato@nuee.nagoya-u.ac.jp).

O. Moriwaki and S. Kamei are with NTT Photonics Laboratories, NTT Corporation, Atsugi, Kanagawa 243-0198, Japan (e-mail:moriwaki@aecl.ntt.co.jp; kamei@aecl.ntt.co.jp).

Color versions of one or more of the figures in this paper are available online at http://ieeexplore.ieee.org.

Digital Object Identifier 10.1109/JLT.2008.929125

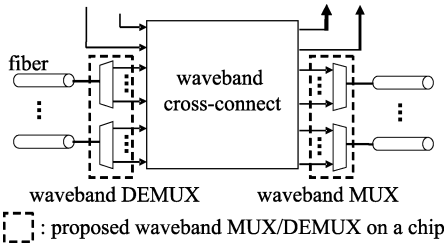

Fig. 1. Configuration of node with multiple input fibers.

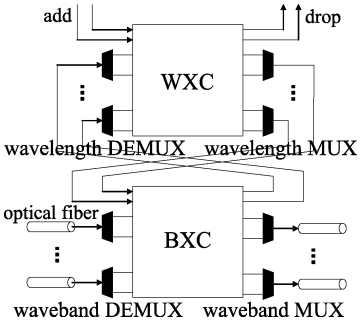

Fig. 2. Generic configuration of HOXC.

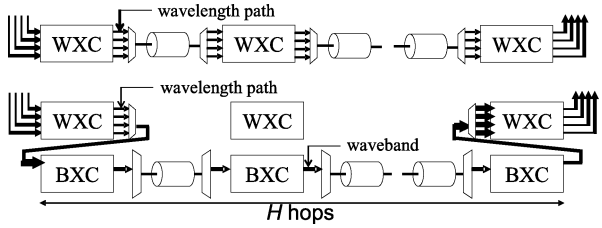

Fig. 3. Port occupation by a waveband in single-layer or hierarchical optical path network.

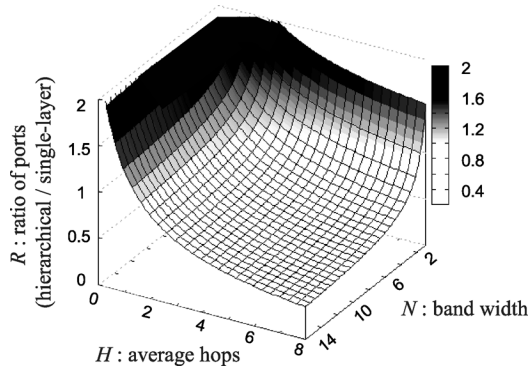

Fig. 4. Ratio of required optical ports between hierarchical and single-layer networks.

consists of two AWGs (wavelength MUX/DEMUX). This filtering effect can be mitigated substantially by using interleavers that double the wavelength spacing.

In this paper, we first briefly discuss the salient background; the effectiveness of hierarchical networks in Section II, and different waveband arrangements in Section III. We then, in Section IV generalize and formulate connection arrangements of the two AWGs of the proposed waveband MUX/DEMUX, which is an extension of our previous works which introduced the basic formulation for cyclic AWGs [20]. Next, after applying the developed formulations, we numerically evaluate and compare the usage of AWG ports for combinations of different types of AWGs and of waveband arrangements. Port utilization, one of the measures used to indicate the device's efficiency, was the subject of a preliminary and very limited report [17]. Next, in Section V, the important characteristic of the coherent and incoherent crosstalk performance of the proposed waveband MUX/DEMUX is discussed. We show how to reduce crosstalk. We then, in Section VI, expand the capability of our proposed waveband MUX/DEMUX to create flexible wavebands through the addition of small switches in combination. Bandwidth flexibility is an attractive attribute that allows cost-effective evolution of the cross-connect system throughput in response to later traffic increases. Finally, in Section VII, some experimental results are introduced to confirm the performance of the proposed waveband MUX/DEMUX. A quick report on the experiments was presented in [19] and [21] by authors.

II. Benefits of Wavebands

In this section, we clarify the potential benefit of introducing wavebands. We assume the hierarchical OXC shown in Fig. 2. It consists of two parts, BXC and WXC. The BXC routes waveband paths and uses the waveband MUX/DEMUX. The WXC routes wavelength paths and uses the wavelength MUX/DEMUX. Fig. 3 schematically illustrates single-layer and hierarchical optical path networks, where only one fiber between nodes is illustrated for simplicity. In a single-layer optical path network, each WXC switch port is allocated on a wavelength path basis and optical paths are routed. On the other hand, in a hierarchical optical path network, multiple wavelength paths are routed as a whole and consume one BXC port of each intermediate node. Therefore, the number of necessary switch ports in a network can be substantially decreased [22]. Fig. 4 demonstrates the degree of total optical cross-connect switch port reduction that is attained by introducing wavebands [22]. The two horizontal axes are the number of wavelength paths per waveband, N, and the average number of hops in the network, H, and the vertical axis is the ratio , R, of total cross-connect switch ports required in hierarchical to those of single-layer optical path network. In Fig. 4, it is assumed that the traffic volume is large enough to fill each end-end waveband path, and all links have utilization rates of almost 1. The effect of traffic volume on R is discussed in [22]. The figure shows that waveband introduction is effective over a wide parameter range of H and N. For example, when H is 4 and N is 8, R is about 0.5. The effectiveness of using wavebands has been proven more precisely by applying a recently developed hierarchical optical path network design algorithm; see [10] for the details.

III. Comparison of Continuous and Interleaved Waveband Arrangement

Fig. 5(a) and (b) depicts two different waveband arrangements. The first one, a conventional arrangement, is the continuous waveband arrangement. Each waveband (WB_k) accommodates continuous wavelength paths ($\lambda_{kN+1} \sim \lambda_{(k+1)N}$) on

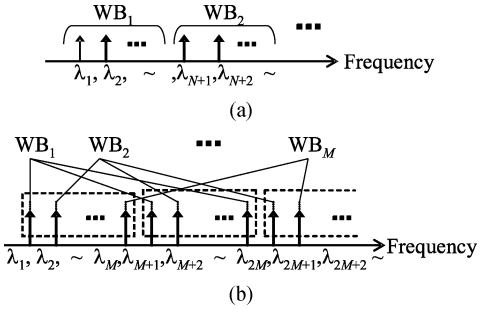

Fig. 5. Two waveband arrangements. (a) Continuous waveband arrangement. (b) Interleaved waveband arrangement.

the ITU-T grid, where N is the number of wavelength paths per waveband.

The other offers the interleaved waveband arrangement. The waveband (WB_k) accommodates interleaved wavelength paths ($\lambda_k, \lambda_{k+M} \sim \lambda_{k+(N-1)M}$) on the ITU-T grid, where N and M are the number of wavelength paths per waveband and wavebands per fiber, respectively. When wavelength paths that are accommodated within a waveband need to be cross connected or terminated at a node, the waveband must be demultiplexed using the wavelength path MUX/DEMUX. The channel spacing between wavelength paths is much wider for an interleaved waveband than for a continuous waveband, so the wavelength path MUX/DEMUX required for an interleaved waveband can be realized with an AWG without any temperature control. The fabrication tolerance is also rather large and the integration of many wavelength MUX/DEMUX devices on a single chip becomes easier (the fabrication error is significantly mitigated). Thus, the interleaved waveband arrangement can ease wavelength MUX/DEMUX fabrication concerns.

The waveband arrangement has virtually no effect in terms of network Operation, Administration, Maintenance, and Provisioning (OAM&P) including network design issues.

IV. Formulation of Port Connections of Two AWGs in Proposed Waveband MUX/DEMUX

The continuous waveband arrangement can eliminate all waveguide crossings that connect the two AWGs. The interleaved waveband arrangement cannot match this attribute, however, it can maximize MUX/DEMUX port utilization efficiency. We explain these attributes using Figs. 6–10.

In our assumed cyclic AWGs with L input and L output ports, the output port number (# output port) corresponding to each pair of wavelength number (# wavelength) and input port number (# input port) is determined by (1).

$$\#\,output\,port = (\#\,wavelength - \#\,input\,port)_{\mathrm{mod}\,L} + 1. \quad (1)$$

Cyclic means that the free spectral range (FSR) of the $L \times L$ AWG equals the width of L channels. Similarly, for wide FSR AWGs (conventional AWGs), # output port corresponding to each pair of # wavelength and # input port is determined by (1a)

$$\#\,output\,port = \#\,wavelength - \#\,input\,port + f \quad (1a)$$

where f is an integer.

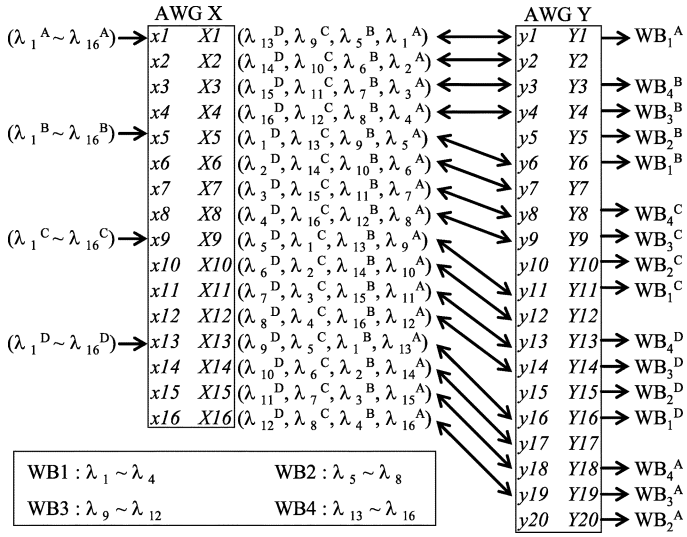

Fig. 6. Continuous waveband MUX/DEMUX that concatenates two cyclic AWGs.

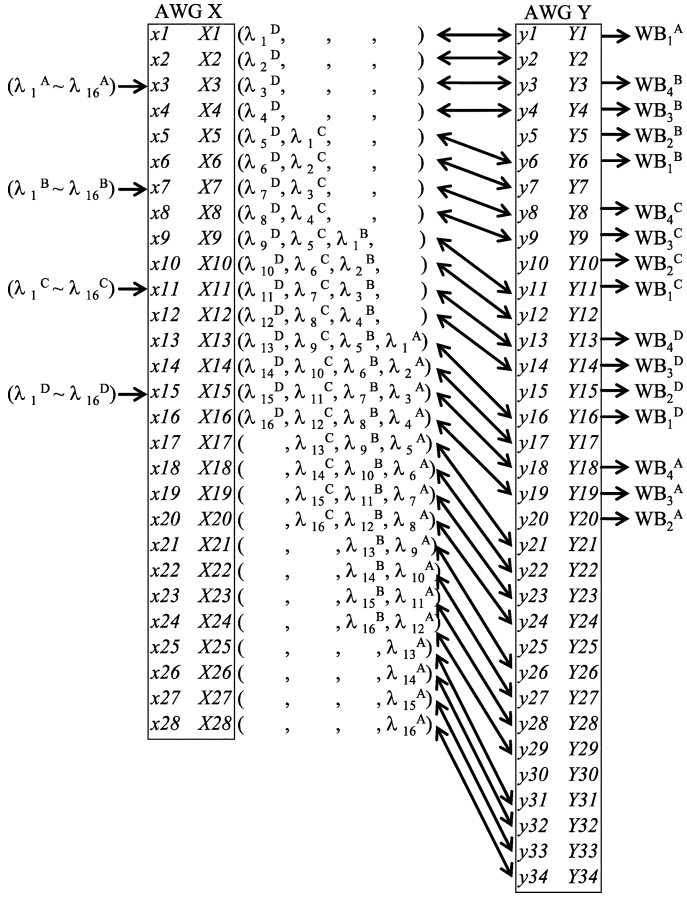

Fig. 7. Continuous waveband MUX/DEMUX that concatenates two conventional AWGs.

There are several possible variations for the AWG used and waveguide connection pattern adopted, and only the most fundamental and effective ones are discussed hereafter. That is, variations that introduce extra AWG ports and increase unused AWG ports are not considered here.

Let L be the maximum number of wavelength paths per fiber, M is the number of wavebands per fiber, and N is the number of wavelength paths per waveband. Hence, the product of M and N is L. We use the following symbols: wavebands $\mathrm{WB_1}^{\mathrm{k}} \sim \mathrm{WB}_M{}^{\mathrm{k}}$ in the kth input fiber, wavelength paths $\lambda_1{}^{\mathrm{k}} \sim \lambda_N{}^{\mathrm{k}}$ in $\mathrm{WB_1}^{\mathrm{k}}$. Input side AWG is denoted as AWG X, and output side AWG, AWG Y, and input/output ports of AWG X and AWG Y, $x1 \sim xa/\,X1 \sim Xa$ and $y1 \sim ya/\,Y1 \sim Ya$ (see Fig. 6).

A. Continuous Waveband MUX/DEMUX Developed With Concatenated Two AWGs

Figs. 6 and 7 are examples of our proposed continuous waveband MUX/DEMUX that concatenates two AWGs, where cyclic and noncyclic AWGs are used, respectively. Assume that kth waveband WB_k ($k = 1 \sim M$) accommodates N wavelength paths $\lambda_{kN+1} \sim \lambda_{(k+1)N}$. Suppose that we have AWG X and AWG Y whose sizes are $S \times S$ and $(S+M) \times (S+M)$, respectively. In this case, the MUX/DEMUX is realized by the following connections between the two AWGs

$$\#y_{\mathrm{in}} = \#X_{\mathrm{out}} + \left\lfloor \frac{(\#X_{\mathrm{out}} - 1)}{N} \right\rfloor + g \qquad (1 \le \#X_{\mathrm{out}} \le S,\ 1 \le \#y_{\mathrm{in}} \le (S+M)) \quad (2)$$

where $\lfloor z \rfloor$ is the largest integer such that $\lfloor z \rfloor \le z$, and $g \in \{0, 1\}$ is a fixed constant. Input fiber connection ports to AWG X can be determined by (3)

$$\#\,x_{\mathrm{in}} = i + jN \quad \left(j = 0, 1, \ldots, \left\lfloor \frac{(S-i)}{2N} \right\rfloor\right) \qquad (3)$$

where i is a fixed integer such that $1 \le i \le S$. In utilizing cyclic AWGs, S is equal to L. In utilizing conventional AWGs, the size of AWG X and Y should be $S \times S$ and $(S+M) \times (S+M)$, that is, determined by the number of input fibers and wavelength paths per fiber. Please note that multiple input fibers that satisfy (3) can be accommodated. With AWG X, the size of which is larger, it is possible to create the waveband MUX/DEMUX, however, port usage is degraded and so it is not discussed here. In Fig. 6, the MUX/DEMUX is realized with two cyclic AWGs that can accommodate 16 wavelength paths per fiber and 4 input fibers (each fiber carries four continuous wavebands, each consisting of 4 wavelength paths), and parameters g and i in (2) and (3) are set at 0 and 1, respectively. In Fig. 7, the MUX/DEMUX is realized with two conventional AWGs that can accommodate 16 wavelength paths per fiber and four input fibers (each fiber carries four continuous wavebands each consists of four wavelength paths), and parameters f, g, and i in (1a), (2) and (3) are set at 15, 0, and 3, respectively. It should be noted that the continuous waveband arrangement can eliminate all waveguide crossing between the two AWGs, which is very attractive for the monolithic realization of the MUX/DEMUX via silica planar lightwave circuit (PLC) technologies. The results of a monolithic realization are presented in Section VII. Please note that with this arrangement, there are some unused AWG Y ports as shown in Figs. 6 and 7. As numerically shown later, the port utilization is better for the waveband MUX/DEMUX that uses cyclic AWGs than one that uses continuous AWGs. However, the maximum frequency error of wavelength channels generally becomes large when smaller FSR AWGs, that is, cyclic AWGs are used. So the arrangement used should be selected considering the required wavelength error specifications.

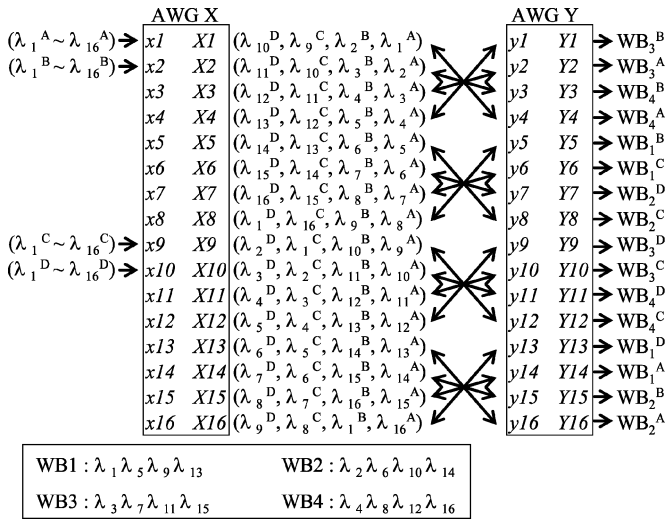

Fig. 8. Interleaved waveband MUX/DEMUX that concatenates two cyclic AWGs.

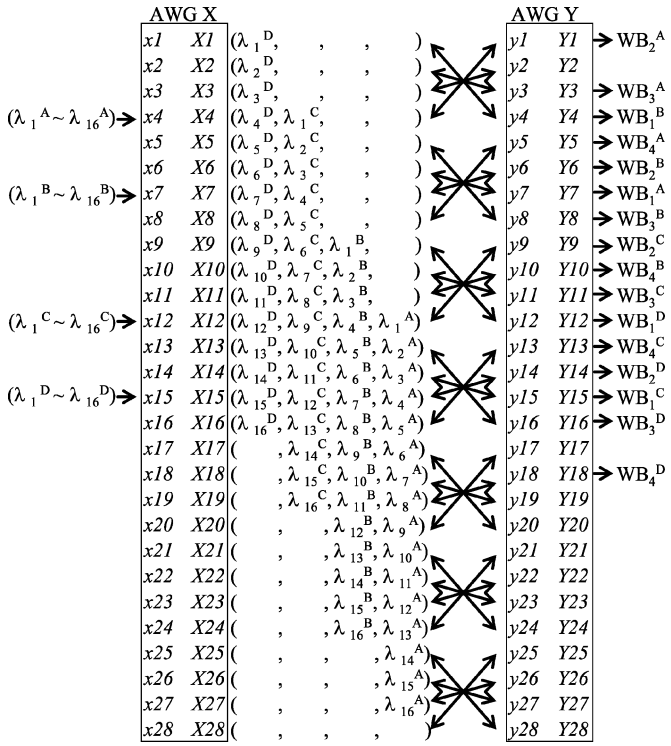

Fig. 9. Interleaved waveband MUX/DEMUX that concatenates two conventional AWGs.

B. Interleaved Waveband MUX/DEMUX Developed With Concatenated Two AWGs

Figs. 8 and 9 show examples of our proposed interleaved waveband MUX/DEMUX developed with two concatenated AWGs. Let kth waveband WB_k ($k = 1 \sim M$) accommodate N wavelength paths λ_k, $\lambda_{k+M} \sim \lambda_{k+(N-1)M}$. Suppose that we have AWG X and AWG Y whose sizes are both $S \times S$. In utilizing cyclic AWGs, S is equal to L. The MUX/DEMUX is

realized by the following connections between the two AWGs, (4) for cyclic AWGs and (4a) conventional AWGs

$$\#y_{\text{in}} = \left\{ M\left(2\left\lfloor \frac{(\#X_{\text{out}}-1)}{M}\right\rfloor +1\right) - \#X_{\text{out}} + g \right\}_{\bmod S} + 1 \qquad (1 \le \#X_{\text{out}} \le S,\ 1 \le \#y_{\text{in}} \le S) \tag{4}$$

$$\#y_{\text{in}} = M\left(2\left\lfloor \frac{(\#X_{\text{out}}-1)}{M}\right\rfloor +1\right) - \#X_{\text{out}} + 1 \qquad (1 \le \#X_{\text{out}} \le S,\ 1 \le \#y_{\text{in}} \le S) \tag{4a}$$

where g is a fixed integer. Input fiber connection ports to AWG X can be determined by

$$\#x_{\text{in}} = 2jM + i \text{ or } \quad 2jM + i + h \quad \left(j = 0, 1, \ldots, \left\lfloor \frac{(S-i)}{2M}\right\rfloor \text{ or } \left\lfloor \frac{(S-i-h)}{2M}\right\rfloor\right) \tag{5}$$

where $h \in \{1, 3, \ldots, 2M-1\}$ is a fixed constant, and i is a fixed integer such that $1 \le i \le S$. In utilizing conventional AWGs, the size of AWG X and Y, $S \times S$, is determined by the number of input fibers and wavelength paths per fiber. In Fig. 8, the MUX/DEMUX is realized with two cyclic AWGs that can accommodate 16 wavelength paths per fiber and 4 input fibers (each fiber carries four interleaved wavebands each consisting of four wavelength paths), and parameters g, i, and h in (4) and (5) are set at 1, 1, and 1, respectively. In Fig. 9, the MUX/DEMUX is realized with two conventional AWGs that can accommodate 16 wavelength paths per fiber and four input fibers (each fiber carries four interleaved wavebands each consisting of four wavelength paths), and parameters f, j, and i in (1a), (4) and (5) are set at 15, 4, and 3, respectively. Compared to the continuous waveband case see Figs. 6 and 7, this interleaved waveband arrangement can enhance AWG port usage because the size of AWG Y for the interleaved waveband MUX/DEMUX is smaller than that for the continuous waveband. However the waveguide crossings between the two AWGs cannot be eliminated.

Another important characteristic is that this MUX/DEMUX permits the connection of multiple bidirectional input fibers. This can maximize the utilization efficiency of the input and output ports of the AWGs. For example, regarding the arrangement shown in Fig. 8, in additional to four input fibers that are connected to AWG X, another set of four input fibers can be connected to AWG Y port *Y3*, *Y4*, *Y11*, and *Y12*, and each waveband on the AWG Y input fibers is demultiplexed and output from AWG X port *xi* as shown in Fig. 10. Please note that with this arrangement, a waveband consisting of λ_4, λ_8, λ_{12}, and λ_{16}, cannot be used. This restriction can be removed by using optical circulators. The circulators, which are not shown in Fig. 10, can be placed at service ports, *x1*, *x2*, *x9*, *x10*, *Y3*, *Y4*, *Y11*, and *Y12*.

As described so far, the interleaved waveband arrangement allows the same scale (port number) AWGs to be used (see Figs. 8–10) and hence the port utilization is enhanced compared to that for the continuous waveband arrangement which requires larger AWG Y than AWG X (compare Figs. 6 and 8, and Figs. 7 and 9). The use of cyclic AWGs can minimize unused ports in AWG X and AWG Y (compare Figs. 6 and 7, and Figs. 8 and 9). The quantitative evaluations of the port utilization are given in Section IV-D. The interleaved arrangement introduces waveguide crossing between AWG X and AWG Y, when two

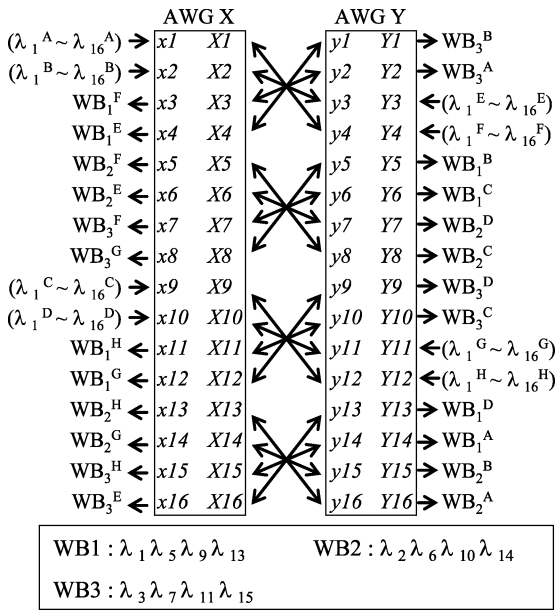

Fig. 10. Waveband MUX/DEMUX for multiple bdirectional input fibers with interleaved waveband arrangement.

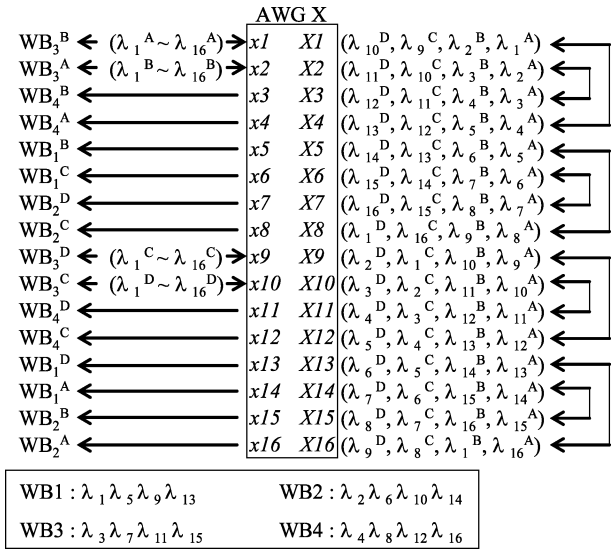

Fig. 11. Interleaved waveband MUX/DEMUX developed on single cyclic AWG.

AWGs are utilized. This waveguide crossing can be eliminated by single AWG arrangement as described in Section IV-C.

C. Interleaved Waveband MUX/DEMUX Developed on Single AWG

The waveband MUX/DEMUX discussed so far requires two AWGs. This means that in monolithic implementation we must minimize the performance variance between the two AWGs. If the single AWG configuration is possible, it will substantially relax fabrication tolerances and increase yields.

Figs. 11 and 12 show a novel interleaved waveband MUX/DEMUX that is realized using just one AWG. Further, the device has none of the waveguide crossings needed to connect the two AWGs. As a result, the interleaved waveband MUX/DEMUX will greatly ease monolithic implementation.

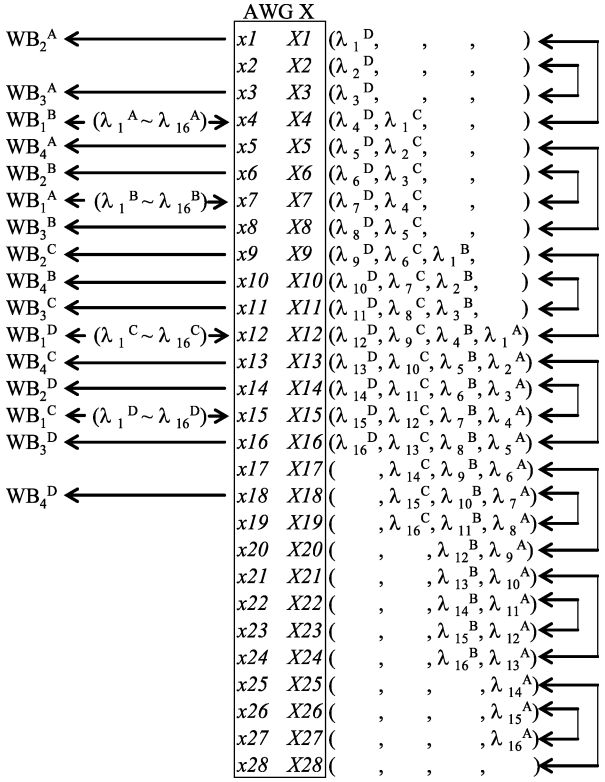

Fig. 12. Interleaved waveband MUX/DEMUX developed on single conventional AWG.

Figs. 11 and 12 show examples of this novel interleaved waveband MUX/DEMUX using a single AWG X. Let kth waveband, WB_k ($k = 1 \sim M$) accommodate N wavelength paths λ_k, $\lambda_{k+M} \sim \lambda_{k+(N-1)M}$. Suppose that we have AWG X of $S \times S$. In this case, the MUX/DEMUX is realized by connecting some of the output ports of AWG X (the right side ports of AWG X) as indicated by (6).

$$\#X_{\mathrm{out}} = M\left(2\left\lfloor\frac{(\#X_{\mathrm{out}}-1)}{M}\right\rfloor+1\right)-\#X_{\mathrm{out}}+1 \quad (1 \le \#X_{\mathrm{out}} \le S). \quad (6)$$

Input fiber connection ports to AWG X can be determined by (5). In utilizing cyclic AWGs, S is equal to L. In utilizing conventional AWGs, the size of AWG X, $S \times S$, depends on the number of input fibers and wavelength paths per fiber. The MUX/DEMUX shown in Fig. 11 which utilizes a cyclic AWG can accommodate 16 wavelength paths per fiber and four input fibers (each fiber carries four interleaved wavebands each consisting of four wavelength paths), and parameters j and i in (5) and (6) are set at 1 and 1, respectively. In Fig. 12, the MUX/DEMUX that utilizes a conventional AWG is shown. It can accommodate 16 wavelength paths per fiber and four input fibers (each fiber carries four interleaved wavebands each consisting of four wavelength paths), and parameters f, j, and i in (1a), (5) and (6) are set at 15, 1, and 1, respectively. Here various different sets of (f, j, i) values are possible. In order to make the suffix values of λ range from 1 to 16, where waveband one consists of λ_1, λ_5, λ_9, and λ_{13}, the specific set of (f, j, i) values is adopted. Please note that the MUX/DEMUX arrangement shown in Figs. 11 and 12 requires optical circulators at some ports (*x1, x2, x9, x10* in Fig. 11, and *x4, x7, x12, x15* in Fig. 12) because some wavebands ($\mathrm{WB_3}^{\mathrm{A,B,C,D}}$ in Fig. 11, and $\mathrm{WB_1}^{\mathrm{A,B,C,D}}$ in Fig. 12) are output from ports to which input fibers are connected. Of course, if you do not use those wavebands, $\mathrm{WB_3}^{\mathrm{A,B,C,D}}$ in Fig. 11, and $\mathrm{WB_1}^{\mathrm{A,B,C,D}}$ in Fig. 12, no circulators are needed.

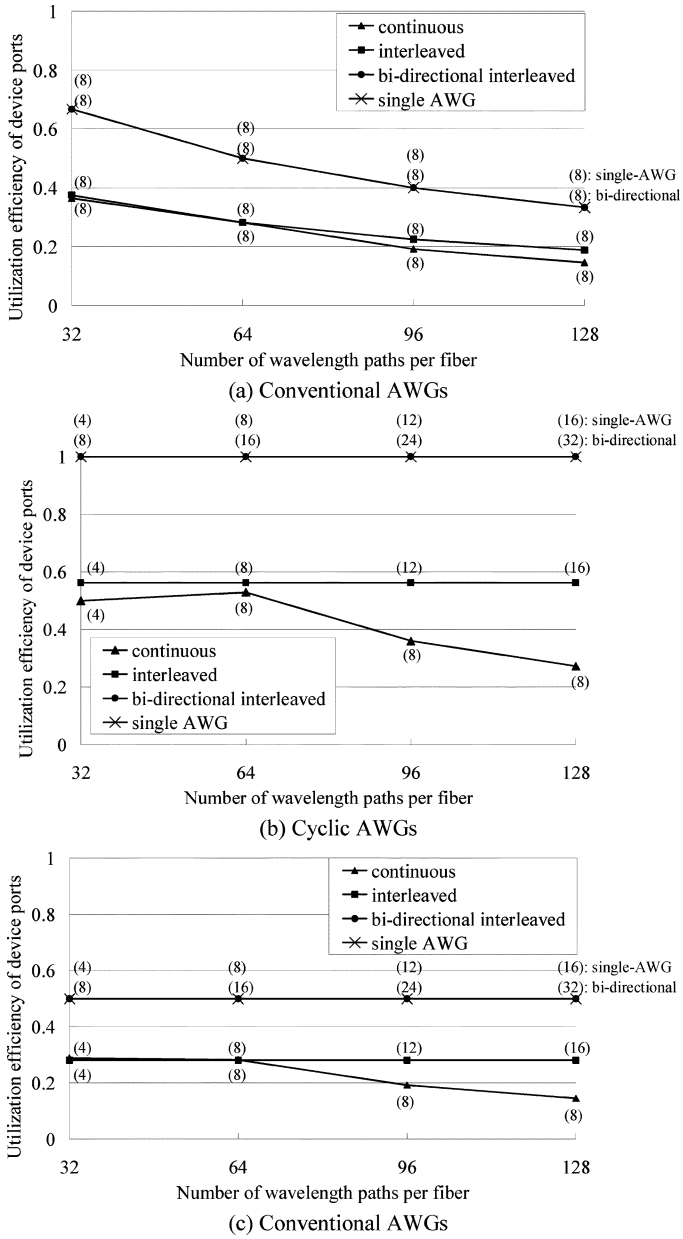

Fig. 13. Utilization efficiency of device port for different waveband MUX/DEMUX arrangements. Number in the parentheses indicates the number of input fibers accommodated. (a) When conventional AWGs are utilized and the number of fibers is eight. (b) When cyclic AWGs are utilized. (c) When conventional AWGs are utilized for the same number of fibers as in (b).

D. Comparison of Port Utilization Efficiencies for the Proposed Waveband MUX/DEMUX

Fig. 13(a)–(c) compares the utilization efficiency of the device ports, defined here as the ratio of number of used ports to

total port number of AWG input and output ports. Here, the number of wavelength paths per fiber is changed and that of wavebands is set at 8. The number in the parentheses denotes the number of input fibers that can be accommodated.

Fig. 13(a) compares port utilization for different waveband MUX/DEMUX arrangements when conventional AWGs are utilized. In this case, the required AWG sizes (and so port utilization) depend on the number of input fibers to be accommodated. In the evaluations, therefore, the number of input fibers is set to be eight for comparison. Bdirectional input fiber waveband MUX/DEMUX and waveband MUX/DEMUX developed on a single AWG yield higher port utilization than others. The interleaved and continuous waveband arrangements are shown to have little impact on the port utilization.

Fig. 13(b) compares port utilization for different waveband MUX/DEMUX arrangements when cyclic AWGs are utilized. In this case, AWG sizes are equal to the number of wavelengths per fiber. Therefore, when cyclic AWGs are utilized, the number of input fibers that can be accommodated is automatically determined by the number of wavelength paths per fiber and that of waveband per fiber (eight in this case). The bdirectional input fiber waveband MUX/DEMUX and waveband MUX/DEMUX developed on a single AWG can maximize the utilization efficiency (100%) of the input and output ports of the AWGs.

Fig. 13(c) compares port utilization when conventional AWGs are utilized for the same number of fibers as in Fig. 13(b). As mentioned above, when conventional AWGs are utilized, the required AWG sizes depend on the number of input fibers to be accommodated. In order to highlight the differences in port utilization between cyclic and conventional AWG case, the number of input fibers is set at the same values as those using cyclic AWGs that are shown in Fig. 13(b). Comparing Fig. 13(b) to (c), it is clear that the port utilization is higher when using cyclic AWGs.

V. Crosstalk Evaluation

One of the most important measures of AWG performance is crosstalk. Because the output waveguides of the AWG are relatively closely spaced, each output signal slightly leaks into the ports neighboring the intended output port. Thus, the waveband MUX/DEMUX using concatenated AWGs can have the same problem. The crosstalk is classified into two groups; one is coherent crosstalk, and the other is adjacent crosstalk.

Coherent crosstalk is the leakage of a signal into neighboring output ports whose output signals share the same frequency. Our proposed continuous waveband MUX/DEMUX has low coherent crosstalk because output signals from neighboring output ports have different frequencies (different frequency waveband). On the other hand, the interleaved waveband MUX/DEMUX shown in Fig. 8 has may have some coherent crosstalk since signals in neighboring output ports lie in the same waveband. This can be avoided by aligning input fiber connection so that no pair of input fibers are adjacent [this can be easily done by checking (1) and (1a)]. Fig. 14 shows an example of the interleaved waveband MUX/DEMUX that can suppress coherent crosstalk without decreasing the utilization efficiency of the device port.

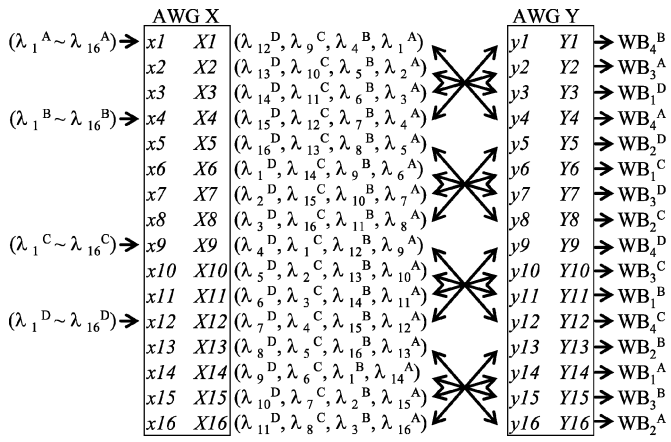

Fig. 14. Interleaved waveband MUX/DEMUX to suppress the coherent crosstalk.

Adjacent crosstalk is the leakage of a signal into neighboring output ports whose output signals have different frequencies. This adjacent crosstalk is, however, eliminated by passing the signal through the waveband MUX that is placed after cross-connect switch and connected to the output fiber [19]. This is because all the adjacent crosstalk is output at the ports other than those used to connect output fibers [19].

Further, the simplest way of suppressing the generation of the adjacent crosstalk to a level that causes no substantial deterioration in signal quality is to adopt the arrangement that prevents any pair of used output ports from being adjacent. For the continuous waveband MUX/DEMUX, the suppression of adjacent crosstalk is realized by the following connections between the two AWGs

$$\#\, y_{\text{in}} = \#\, X_{\text{out}} + 2\left\lfloor \frac{(\#\, X_{\text{out}} - 1)}{N} \right\rfloor + g \qquad (1 \le \#\, X_{\text{out}} \le S,\ 1 \le \#\, y_{\text{in}} \le (S+M)) \quad (7)$$

where $g \in \{0,1\}$ is a fixed constant. For the interleaved waveband MUX/DEMUX, the suppression can be realized by the following connections of input fibers

$$\#\, x_{\text{in}} = 2jM + i \quad \left(j = 0, 1, \ldots, \left\lfloor \frac{(S-i)}{2M} \right\rfloor\right) \quad (8)$$

where i is a fixed integer such that $1 \le i \le S$. Figs. 15 and 16 are examples of the continuous and interleaved waveband MUX/DEMUXs that can suppress the adjacent crosstalk, respectively. This arrangement yields less efficient port usage of course.

VI. Flexible Bandwidth MUX/DEMUX

Flexibility in allocation of bandwidth in waveband MUX/DEMUX is attractive since it allows cost-effective evolution of the cross-connect system throughput in response to subsequent traffic increases. In this section, examples of flexible waveband MUX/DEMUXs are presented that can be realized with our proposed waveband MUX/DEMUX and small switches. Figs. 17 and 18 show examples of the flexible waveband MUX/DEMUX utilizing four 4×4 switches. The number of wavebands per fiber can be varied by changing the switch settings (represented

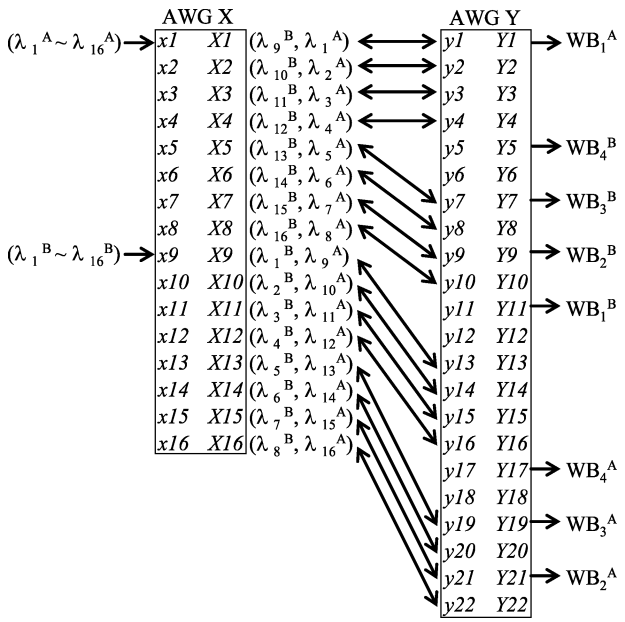

Fig. 15. Continuous waveband MUX/DEMUX to reduce the adjacent crosstalk.

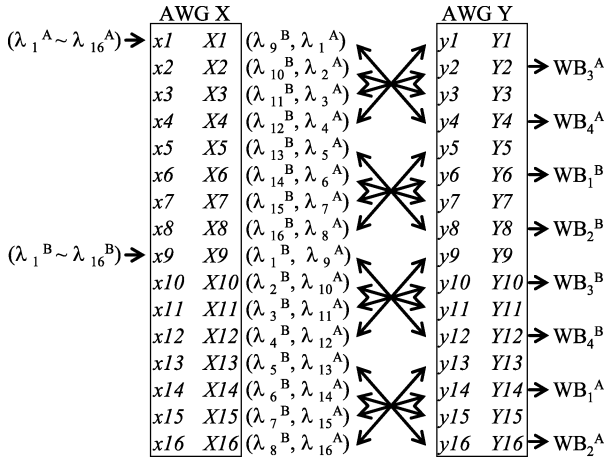

Fig. 16. Interleaved waveband MUX/DEMUX to reduce the adjacent crosstalk.

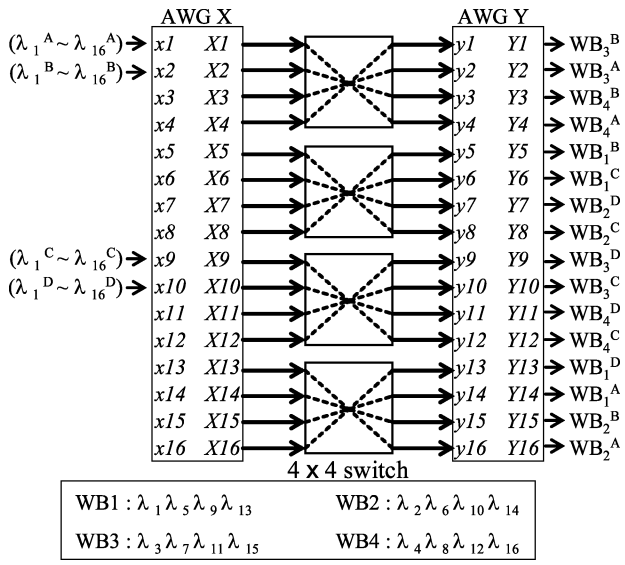

Fig. 17. Flexible waveband MUX/DEMUX de/multiplexing four wavebands.

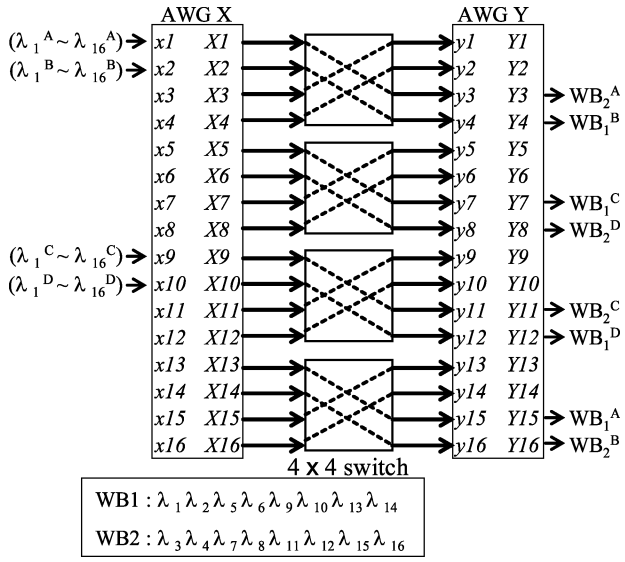

Fig. 18. Flexible waveband MUX/DEMUX de/multiplexing two wavebands.

by dotted lines). The switch setting shown in Fig. 17 classifies 16 wavelengths in each fiber into four wavebands each consisting of four wavelength paths. The switch setting shown in Fig. 18 classifies 16 wavelengths in each fiber to 2 wavebands each consisting of 8 wavelength paths. When different combinations of the AWGs and switches are used, different flexibilities are realized. This flexibility ensures the cost-effective introduction of BXC because the number of wavebands per fiber can be set in accordance with the traffic.

VII. Experiments

A. Continuous Waveband MUX/DEMUX

Waveband MUX/DEMUXs utilizing cyclic AWGs were shown to increase the port utilization efficiency. However, there is a problem with cyclic AWGs. It is inherently difficult to precisely align the center frequency of each channel on the ITU-T grid among the multiple wavebands; frequency deviation causes transmission signal distortion and large optical loss, particularly at or close to the edge channels of each waveband, and for wavebands near the edge of the total band (i.e., C or/and L-band). The use of conventional AWG can relax this problem, but it lowers port utilization efficiency as discussed earlier. The deviations for conventional AWGs depend on the wavelength range used, that is, channel spacing multiplied by channel number. For example, conventional C-band AWG (nearly 100 GHz $\times$ 40 ch) produces about $+/-10$ GHz deviations at the C-band edges, which will be acceptable for most known applications. When the spectral range is expanded to the C+L band, the deviation will become an issue. Two separate AWGs may then be required to cover the band.

In order to verify the basic performance of our proposed device, we first fabricated a continuous waveband MUX/DEMUX on a chip using wide FSR AWGs (same FSR for the two

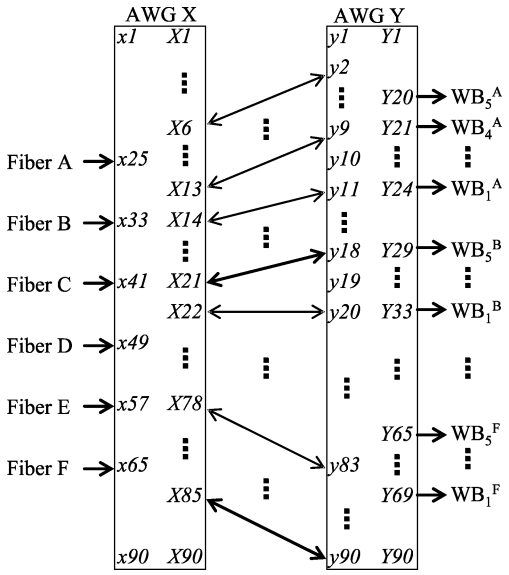

Fig. 19. Fabricated waveband MUX/DEMUX utilizing wide FSR AWGs.

TABLE I
CHIP PARAMETERS.

size	3 x 7 cm^2
# of waveguide connections	80
# of input fibers	6
# of wavelength channels per fiber	40 (191.8 + 0.1 x n [THz]; n = 0 ~ 39)
total # of wavelength channels	40 x 6 = 240
waveguide cross-section dimensions	4.5 μm x 4.5 μm
index contrast	1.5%
frequency error	≤ ±15 GHz
average insertion loss	3.83 dB
worst coherent crosstalk	-34.0 dB

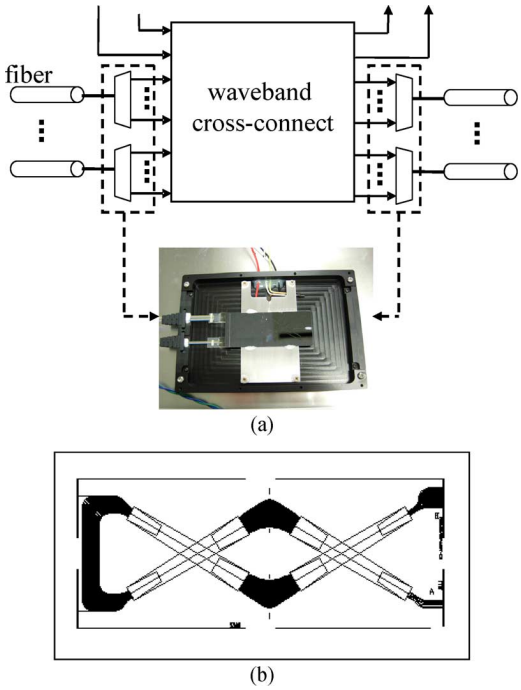

Fig. 20. (a) Device module. (b) Chip layout.

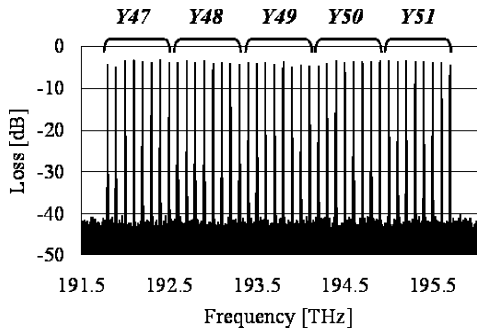

Fig. 21. Output channel spectra at output ports *Y47*, *Y48*, *Y49*, *Y50*, and *Y51*, when six input fibers are connected to ports of *x25*, *x33*, *x41*, *x49*, *x57*, and *x65*.

AWGs) fabricated with silica PLC Technology. Fig. 19 depicts the connection arrangement of the fabricated waveband MUX/DEMUX [19]. Table I summarizes important parameters of the chip. The device can support six input fibers simultaneously, each carrying 40 wavelength channels on the ITU-T grid ($191.8 + 0.1 \times n$ [THz]; $n = 0 \sim 39$). A photo of the developed module is shown in Fig. 20(a) and the chip layout is shown in Fig. 20(b). This compact, reliable and cost-effective waveband MUX/DEMUX will enable cost-effective waveband cross connects.

Fig. 21 shows examples of output channel spectra of the wavebands at output ports *Y47*, *Y48*, *Y49*, *Y50*, and *Y51*, when six fibers were connected to ports *x25*, *x33*, *x41*, *x49*, *x57*, and *x65* (each fiber carries 40-channels). This figure shows that the device retains multi/demultiplexing granularity at the individual wavelength channel level while outputting wavebands at different ports. Outputs from other waveband output ports, Y_{ij}, were also measured and the routing capability of the fabricated device was confirmed to be accurate as designed. The measured average fiber-to-fiber insertion loss was 3.83 dB. The worst and average coherent crosstalk was less than -34.0 and -39.5 dB, respectively, when six input fibers were connected simultaneously. The allowable maximum coherent crosstalk that limits the optical power penalty at the bit error rate of 10^{-9} to within 1 dB is -25 dB [23]. If we expect the maximum node number that can be transparently traversed is 16, which is the typical specification of present ring networks, the maximum total number of MUX and DEMUX traversed is 32. This causes 15-dB crosstalk degradation for the worst case. Thus, the specification for each MUX/DEMUX is -40 dB for this application. The specification depends on the specific number of nodes traversed. The device fabricated here produces the level acceptable for this application. The adjacent band crosstalk is relatively high compared to the coherent crosstalk levels at the output ports. This is because the adjacent band leaks from the neighboring output ports (explained in Section V). The worst adjacent crosstalk at the output port was about -20 dB. This adjacent crosstalk is, however, eliminated when the signal passes through the waveband MUX after the waveband cross-connect switch (see Fig. 20).

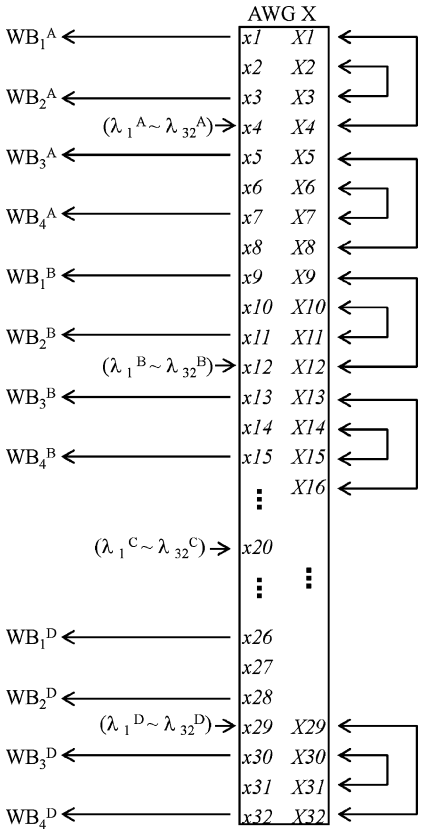

Fig. 22. The arrangement of the constructed interleaved MUX/DEMUX.

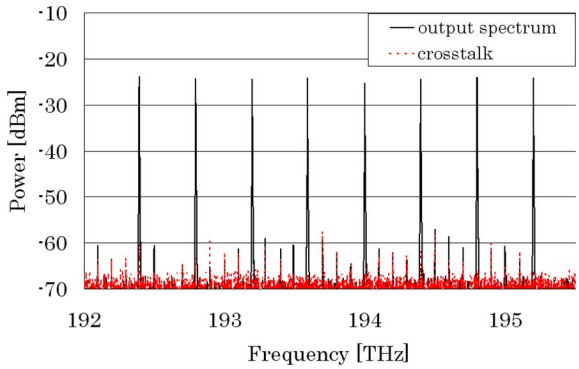

Fig. 23. Output spectrum of one waveband.

B. Interleaved Waveband MUX/DEMUX

The proposed interleaved waveband MUX/DEMUX developed on single AWG will be realized monolithically using silica PLC technology. To confirm device feasibility we constructed a prototype of the interleaved waveband MUX/DEMUX. In the experiment, a 32×32 uniform-loss and cyclic frequency (ULCF [24]) AWG was used, and the 16 pairs of the 32 output ports were connected using 16 optical fibers. The arrangement is shown in Fig. 22. The device can accommodate 32 100-GHz spaced C-band channels (192.1 $\sim$ 195.2 THz) on the ITU-T grid per fiber and four input fibers simultaneously. Each fiber carries four interleaved wavebands with eight channels. Fig. 23 shows an example of a measured output spectrum for the device at output port $x1$. The solid and dotted traces correspond to the output spectrum when four input fibers and three input fibers were connected, respectively; that is, the dotted trace corresponds to crosstalk. Outputs from other waveband output ports were also measured and the routing capability of the prototype device was confirmed to be accurate. The measured worst and average coherent crosstalk values were -36 and -42.0 dB, respectively. The average 3-dB transmission bandwidth was 38 GHz. The average 3 and 1 dB transmission bandwidth (Gaussian) of the used ULCF AWG [24] was 55 GHz and 32 GHz, respectively. The loss of this prototype device was large (more than 10 dB) since we simply used an available ULCF AWG to verify the routing capability. The expected loss of a monolithically fabricated proposed waveband MUX/DEMUX is better than 3.8 dB, since this value has been attained by a monolithically fabricated continuous waveband MUX/DEMUX as explained previously. Characteristics of a recently developed cyclic AWG are presented in [25].

VIII. Conclusion

We developed and analyzed a new waveband MUX/DEMUX that exploits AWG routing functionality. The salient feature of the device is that it can accommodate multiple input fibers simultaneously and be implemented monolithically using silica PLC technology. We formulated the connection patterns of waveguides between AWG input/output ports. Applying the developed formulations, we numerically evaluated and compared AWG port utilization efficiencies for combinations of different types of AWGs and of waveband arrangements. We also investigated the crosstalk characteristics of the devices and elucidated low crosstalk arrangements. Based on the detailed investigations performed herein, we can choose an architecture that matches the specification applications. The capability of our proposed waveband MUX/DEMUX was shown to be enhanced by the addition of small scale switches which yield flexibility in waveband bandwidth setting. This is an attractive characteristic that allows cost-effective evolution of the cross-connect system throughput in response to subsequent traffic increases. Finally, we introduced experimental results that confirm the performance of the proposed waveband MUX/DEMUX. The proposed device is expected to play an important role in creating cost-effective and compact waveband cross-connect systems.

References

[1] D. Cooperson, "ROADM deployment plans in LH and metro networks," in *Proc. OFC/NFOEC*, Mar. 2005, NThK3.

[2] S. Okamoto, T. Otani, W. Imajuku, D. Shimazaki, M. Hayashi, K. Ogaki, M. Miyazawa, I. Nishioka, M. Nanba, K. Morita, S. Kano, S. Seno, K. Sagara, N. Arai, and H. Ohtsuki, "Nationwide GMPLS field trial using different types (MPLS/TDM/Lambda) of switching capable equipment from multiple vendors," in *Proc. OFC/NFOEC*, Mar. 2005, PDP40.

[3] L. Noirie, C. Blaizot, and E. Dotaro, "Multi-granularity optical cross-connect," in *Proc. ECOC*, Oct. 2000, vol. 3, pp. 269–270.

[4] K. Harada, K. Shimizu, T. Kudou, and T. Ozeki, "Hierarchical optical path cross-connect systems for large scale WDM networks," in *Proc. OFC/NFOEC*, Feb. 1999, pp. 356–358.

[5] J. Yamawaku, A. Takada, W. Imajuku, and T. Morioka, "Evaluation of amount of equipment on single-layer optical paths," *J. Lightw. Technol.*, vol. 23, no. 6, pp. 1971–1978, Jun. 2005.

[6] K. Sato, "Recent developments in and challenges of photonic networking technologies," *IEICE Trans. Commun.*, vol. E90-B, no. 3, pp. 454–467, Mar. 2007.

[7] S. Kakehashi, H. Hasegawa, and K. Sato, "Optical switch architectures for hierarchical optical path networks," in *Proc. SPIE Opt. East*, Oct. 2006, vol. 6388, pp. 638809-1–638809-9.
[8] R. Parthiban, R. S. Tucker, and C. Leckie, "Waveband grooming and IP aggregation in optical networks," *J. Lightw. Technol.*, vol. 21, no. 11, pp. 2476–2488, Nov. 2003.
[9] X. Cao, V. Anand, and C. Qiao, "Waveband switching in optical networks," *IEEE Commun. Mag.*, vol. 41, no. 4, pp. 105–112, Apr. 2003.
[10] I. Yagyu, H. Hasegawa, and K. Sato, "An efficient hierarchical optical path network design algorithm based on a traffic demand expression in a cartesian product space," in *Proc. ECOC*, Sep. 2006, vol. 2, pp. 113–114.
[11] X. Cao, V. Anand, Y. Xiong, and C. Qiao, "A study of waveband switching with multilayer multigranular optical cross-connects," *IEEE J. Sel. Areas Commun.*, vol. 21, no. 7, pp. 1081–1095, Sep. 2003.
[12] P.-H. Ho, H. T. Mouftah, and J. Wu, "A scalable design of multigranularity optical cross-connects for the next generation optical internet," *IEEE J. Sel. Areas Commun.*, vol. 21, no. 7, pp. 1133–1142, Sep. 2003.
[13] R. Izmailov, S. Ganguly, V. Kleptsyn, and A. C. Varsou, "Non-uniform waveband hierarchy in hybrid optical networks," in *Proc. IEEE INFOCOM*, Mar. 2003, vol. 2, pp. 1344–1354.
[14] G. J. Ockenfuss, N. A. O'Brien, and E. Williams, "Ultra-low stress coating process: An enabling technology for extreme performance thin film interference filters," in *Proc. OFC/NFOEC*, Mar. 2002, PDFA8.
[15] C. R. Doerr, R. Pafchek, and L. W. Stulz, "Integrated band demultiplexer using waveguide gratings routers," *IEEE Photon. Technol. Lett.*, vol. 15, no. 8, Aug. 2003.
[16] S. Chandrasekhar, C. R. Doerr, and L. L. Buhl, "Flexible waveband optical networking without guard bands using novel 8-skip-0 banding filters," *IEEE Photon. Technol. Lett.*, vol. 17, no. 3, pp. 579–581, Mar. 2005.
[17] S. Kakehashi, H. Hasegawa, K. Sato, and O. Moriwaki, "Waveband MUX/DEMUX using concatenated arrayed-waveguide gratings," in *Proc. ECOC*, Sep. 2006, vol. 3, pp. 233–234.
[18] S. Kakehashi, H. Hasegawa, K. Sato, O. Moriwaki, S. Kamei, Y. Jinnouchi, and M. Okuno, "Waveband MUX/DEMUX using concatenated AWGs –Formulation of waveguide connection and fabrication," in *Proc. OFC/NFOEC*, Mar. 2007, JThA94.
[19] S. Kakehashi, H. Hasegawa, K. Sato, O. Moriwaki, S. Kamei, Y. Jinnouchi, and M. Okuno, "Performance of waveband MUX/DEMUX using concatenated AWGs," *IEEE Photon. Technol. Lett.*, vol. 19, no. 16, pp. 1197–1199, Aug. 15, 2007.
[20] S. Kakehashi, H. Hasegawa, K. Sato, and O. Moriwaki, "Formulation of waveguide connection for waveband MUX/DEMUX using concatenated arrayed-waveguide gratings," *IEICE Trans. Commun.*, vol. E90-B, no. 10, pp. 2950–2952, Oct. 2007.
[21] S. Kakehashi, H. Hasegawa, K. Sato, and O. Moriwaki, "Interleaved waveband MUX/DEMUX developed on single arrayed-waveguide grating," in *Proc. OFC/NFOEC*, Feb. 2008.
[22] K. Sato and H. Hasegawa, "Prospects and challenges of multi-layer optical networks," *IEICE Trans. Commun.*, vol. E90-B, no. 8, Aug. 2007.
[23] H. Takahashi, K. Oda, and H. Toba, "Impact of crosstalk in an arrayed-waveguide multiplexer on $N \times N$ optical interconnection," *J. Lightw. Technol.*, vol. 14, no. 6, pp. 1097–1105, Jun. 1996.
[24] K. Okamoto, T. Hasegawa, O. Ishida, A. Himeno, and Y. Ohmori, "32×32 arrayed-waveguide grating multiplexer with uniform loss and cyclic frequency characteristics," *IEE Electron. Lett.*, vol. 33, pp. 1865–1866, Oct. 1997.
[25] K. Ishii, H. Hasegawa, K. S. Kamei, H. Takahashi, and M. Okuno, "Monolithically integrated waveband selective switch using cyclic AWGs," in *Proc. ECOC 2008*, Belgium, Sep. 2008, Mo.4.C.5.

Shoji Kakehashi was born in 1983. He received the B.E. and M.E. degrees from Nagoya University, Nagoya, Japapn, in 2006 and 2008, respectively.

In 2008, he joined Chubu Electric Power Co., Inc. His major interests include photonic network node architecture, wavelength routing devices, and the optical performances.

Mr. Kakehashi is a member of the IEICE of Japan.

Hiroshi Hasegawa (M'05) received the B.E., M.E., and D.E. degrees, all in electrical and electronic engineering, from the Tokyo Institute of Technology, Tokyo, Japan, in 1995, 1997, and 2000, respectively.

From 2000 to 2005, he was an Assistant Professor of the Department of Communications and Integrated Systems, Tokyo Institute of Technology. Currently, he is an Associate Professor of Nagoya University, Nagoya, Japan. His current research interests include photonic networks, image processing (especially superresolution), multidimensional digital signal processing, and time-frequency analysis.

Dr. Hasegawa received the Young Researcher Awards from the Society of Information Theory and its Applications (SITA) and the Institute of Electronics, Information and Communication Engineers (IEICE) in 2003 and 2005, respectively. He is a member of the IEICE and SITA.

Ken-Ichi Sato (M'87-SM'95-F'99) received the B.S., M.S., and Ph.D. degrees in electronics engineering from the University of Tokyo, Tokyo, Japan, in 1976, 1978, and 1986, respectively.

He is currently a Professor with the Graduate School of Engineering, Nagoya University, Nagoya, Japan, and is also an NTT R&D Fellow. Before joining the university in April 2004, he was an Executive Manager of the Photonic Transport Network Laboratory, NTT, Kanagawa, Japan. His R&D activities cover future transport network architectures, network design, operation administration and maintenance (OA&M) systems, photonic network systems including optical cross-connect/ADM and photonic IP routers, and optical transmission technologies. He has authored/coauthored more than 200 research publications in international journals and conferences. He holds 35 granted patents and more than 100 pending patents. He authored a book *Advances in Transport Network Technologies* (Norwood, MA: Artech House, 1996), and is coauthoring 13 other books.

Dr. Sato received the Young Engineer Award in 1984, the Excellent Paper Award in 1991, and the Achievement Award in 2000 from the Institute of Electronics, Information and Communication Engineers (IEICE) of Japan. He was also the recipient of the Distinguished Achievement Award of the Ministry of Education, Science and Culture in 2002. His contributions to the asynchronous transfer mode (ATM) and optical network technology development extend to coediting three IEEE JOURNAL ON SELECTED AREAS IN COMMUNICATIONS Special Issues and the JOURNAL OF LIGHTWAVE TECHNOLOGY Special Issue once. He organized several Workshops and Conference technical sessions and served on numerous committees of international conferences including OFC and ECOC. He is a Fellow of the IEICE of JAPAN and a Fellow of the IEEE.

Osamu Moriwaki (M'04) was born in Tokyo, Japan, in 1975. He received the B.E. and M.E. degrees in electrical engineering from the University of Tokyo in 1998 and 2000, respectively.

He joined NTT Photonics Laboratories, Kanagawa, Japan, in 2000, where he has been engaged in research on wavelength routing devices.

Mr. Moriwaki is a member of the Institute of Electronics, Information, and Communication Engineers (IEICE) of Japan.

Shin Kamei was born in Saitama, Japan, on September 19, 1972. He received the B.S. and M.S. degrees in physics from the Tokyo Institute of Technology, Tokyo, Japan, in 1996, and 1998, respectively.

He joined NTT Photonics Laboratories, Kanagawa, Japan, in 1998, where he has been engaged in research on silica-based planar lightwave circuits (PLCs).

Mr. Kamei is a member of the Institute of Electronics, Information and Communication Engineers (IEICE) of Japan.